J. Geomag. Geoelectr., **45**, 833–839, 1993

Mohr Circles in Magnetotelluric Interpretation (i) Simple Static Shift; (ii) Bahr's Analysis

F. E. M. (Ted) LILLEY

Research School of Earth Sciences, Australian National University, Canberra 0200, Australia

(Received December 17, 1992; Revised March 15, 1993; Accepted March 15, 1993)

Mohr circles drawn for magnetotelluric impedance data show particular patterns which may be a guide in the choice of models taken for interpretation. Data affected by local static shift over a one-dimensional structure will generate circles which lie in distinctive envelopes, indicating an anisotropy which is of two-dimensional appearance and which is constant for both real and quadrature parts, at all frequencies.

For three-dimensional data, Mohr circles show the skew angles defined by Bahr, once Bahr's rotation angles are known. For strong distortion or high anisotropy, the 90° relationship between Bahr's skew angles is evident on a Mohr circle.

1. Introduction

This paper explores two different aspects of Mohr circles in magnetotelluric analysis, as an aid to the recognition of particular geological circumstances. The two situations examined are one-dimensional (1D) data distorted by simple "static-shift"; and, for three-dimensional (3D) data, evidence given by the circles for the parameters which arise in the analysis described by BAHR (1988, 1991). The construction of such Mohr circles for magnetotelluric data is first described, for reference.

Taking the real parts

$$\begin{bmatrix} Zxx_r & Zxy_r \\ Zyx_r & Zyy_r \end{bmatrix}$$

of a magnetotelluric impedance tensor

$$\begin{bmatrix} Zxx & Zxy \\ Zyx & Zyy \end{bmatrix}$$

axes are drawn for $Z'xy_r$ (abscissa) and $Z'xx_r$ (ordinate), the dash superscript indicating the value of the appropriate tensor element after the observing axes have been rotated clockwise by angle θ'.

A circle is then drawn with its centre at the point

$$Z'xy_r = \frac{1}{2}\left(Zxy_r - Zyx_r\right),$$

$$Z'xx_r = \frac{1}{2}\left(Zxx_r + Zyy_r\right)$$

and with radius

$$R = \frac{1}{2}\left[(Zxx_r - Zyy_r)^2 + (Zxy_r + Zyx_r)^2\right]^{1/2}.$$

The radius drawn from the centre to the originally observed point (Zxy_r, Zxx_r) then forms a reference arm. Rotation of this arm anticlockwise by angle $2\theta'$ positions its outer end at the point $(Z'xy_r, Z'xx_r)$; that is, at the values given by rotation of the measuring axes clockwise by angle θ'.

As shown in LILLEY (1976, 1993), for one-dimensional data the circle is simply a point on the $Z'xy_r$ axis; for two-dimensional data the circle has its centre on the $Z'xy_r$ axis; and for three-dimensional data the circle centre moves off the $Z'xy_r$ axis.

In addition to the $Z'xy_r$ and $Z'xx_r$ axes as in Fig. 1 of this paper, it may also be informative to include on a Mohr circle diagram the $Z'yx_r$ and $Z'yy_r$ axes, as in Fig. 2 of this paper and as used in the discussion of the BAHR analysis. The $Z'yx_r$ and $Z'yy_r$ axes may be drawn on the same figure as a consequence of the relationships given in LILLEY (1976) that

$$Z'yx_r = Z'xy_r + (Zyx_r - Zxy_r)$$

and

$$Z'yy_r = -Z'xx_r + (Zxx_r + Zyy_r)$$

where the terms $(Zyx_r - Zxy_r)$ and $(Zxx_r + Zyy_r)$ are invariant under rotation.

The above description is for the real parts of tensor elements considered separately, and a similar description applies to the quadrature parts of tensor elements considered separately. In this paper, such quadrature parts will be denoted by subscript q.

Mohr circles enable an assessment of observed data. They are not in themselves a process of data reduction or data inversion, and they do not rely on modelling. An example of their use may be in the correction of observed data for distortion, when data which have been corrected to be ideally 1D or 2D may be checked visually, using Mohr circles, to see how closely they conform to such ideals. Otherwise, the parameters involved in magnetotelluric data may be so numerous as to be difficult to assess together.

2. Simple Static Shift of 1D Data

A simple form of static shift is the local perturbation of 1D data to make it appear 2D, by frequency-independent real factors g and h. That is, for a 1D response Zxy, static shift may take the form

$$\begin{bmatrix} Ex \\ Ey \end{bmatrix} = \begin{bmatrix} g & 0 \\ 0 & h \end{bmatrix} \begin{bmatrix} 0 & Zxy \\ -Zxy & 0 \end{bmatrix} \begin{bmatrix} Hx \\ Hy \end{bmatrix}$$

where here the measuring axes for the x and y components have been taken as those of the perturbing geology.

As shown in Fig. 1a, such a perturbation changes the single point on the $Z'xy_r$ axis at Zxy_r to two points, at $gZxy_r$ and $hZxy_r$, which thus mark the diameter of what now becomes a full Mohr circle. Denoting angle λ (as marked) the anisotropy angle, this angle is given by

$$\lambda = \arctan\left[\frac{1}{2}(g-h)/(gh)^{1/2}\right]$$

and it is thus independent of the impedance and of frequency. Hence all real and quadrature Mohr circles for such a site will lie within the envelopes defined by λ, as shown for a hypothetical data set in Fig. 1b.

Actual data giving the distinctive pattern of Fig. 1b should thus alert an interpreter to the likelihood that the data are static-shifted 1D. Note that the pattern will still hold if data are normalized by multiplication by $T^{1/2}$ (to balance a reduction with increasing period as occurs

over a uniform half-space). Such scaling will have an effect similar to multiplying both g and h by $T^{1/2}$, thus leaving the value of λ unchanged.

The interpretation of such data in terms of 1D models is then based, in effect, on reducing each circle in Fig. 1b to a single point on the $Z'xy_r$ or $Z'xy_q$ axis. Here procedures for the removal of static shift must be addressed by methods as discussed, for example, by JONES (1988). Note that only if

$$g + h = 2$$

will the circle centre be the correct point after correction for static shift. Quite generally, the point Zxy_r may lie outside the circle.

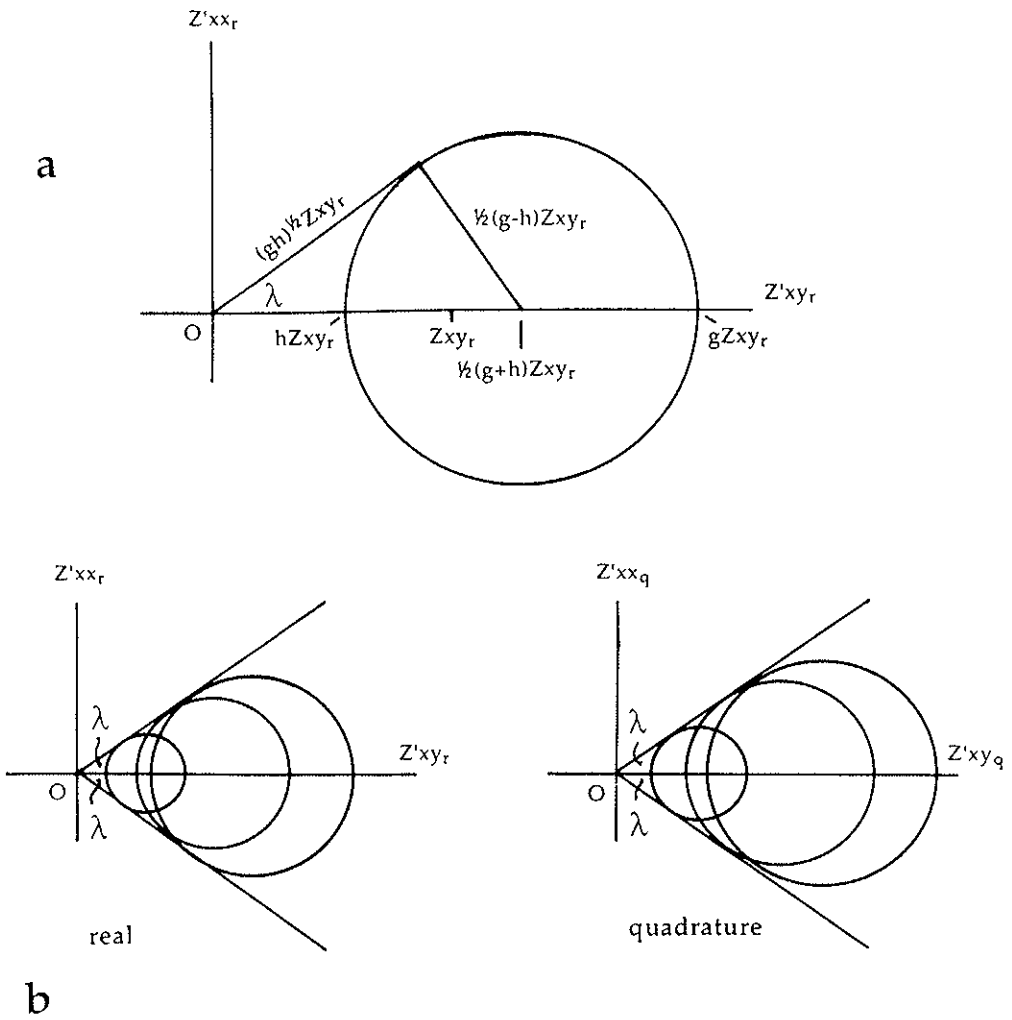

Fig. 1. (a) Effect of static shift changing a (1D) single point Zxy_r to two points $gZxy_r$ and $hZxy_r$, which thus mark the diameter of a full Mohr circle. Note the centre of the circle is not at the original point Zxy_r. A similar effect will occur for the quadrature value, Zxy_q. (b) Envelopes of constant anisotropy λ in which will lie all 1D tensors affected by the same static shift. The patterns show a range of circles, corresponding to a range of frequencies for which magnetotelluric impedance tensors have been determined.

3. The Bahr Rotation and Skew Angles

BAHR (1988, 1991) describes a method for decoupling local and regional anomalies, where the local effect is frequency-independent distortion (that is, general static shift), and the regional effect is regular 2D induction. The method is based on rotating a (general) complex impedance tensor, to obtain two magnetic field directions for which the electric fields are linearly polarized; Bahr calls these two electric fields the "telluric vectors". In the general case, the magnetic field directions are not necessarily orthogonal to each other, and the electric field directions are not orthogonal to each other or to the magnetic field directions.

For the particular case of local distortion of regional 2D induction, the two magnetic field directions will be orthogonal (within some tolerance limit), and will be taken to define regional geologic strike. One direction is taken as being along strike, and the other across strike. Bahr uses vertical component fluctuation information to distinguish which is which, and specifies a regional skew parameter (η in BAHR, 1991) which, as a quantitative measure of the degree of orthogonality of the two magnetic field directions, is also a quantitative measure of the degree of regional two-dimensionality.

The two rotation angles (α) sought for the complex impedance tensor, to align the measuring axes along and across regional strike, are determined by satisfaction of the condition (BAHR, 1988) that

$$\frac{Z'xx_r}{Z'yx_r} = \frac{Z'xx_q}{Z'yx_r}. \tag{1}$$

At such rotations, the telluric vectors depart from orthogonality with their associated magnetic field direction by angular deviations β_1 and β_2 given by (BAHR, 1991)

$$\tan\beta_1 = \frac{-Z'xx_r}{Z'yx_r} = \frac{-Z'xx_q}{Z'yx_q}, \tag{2}$$

$$\tan\beta_2 = \frac{Z'yy_r}{Z'xy_r} = \frac{Z'yy_q}{Z'xy_q} \tag{3}$$

where β_1 and β_2 are also referred to as skew angles.

Figure 2a shows how one of the two values of α will appear on a Mohr circle diagram, with its related angles β_1 and β_2. The rotation of the radial arm through 2α to the point $\theta' = 2\alpha$ is the same rotation which will bring the quadrature circle for the impedance tensor (not shown) to the same value for the ratio $-Z'xx_q/Z'yx_q$, giving also the same values of β_1 and β_2. The angles β_1 and β_2 are as specified in Eqs. (2) and (3).

Circles for an actual impedance tensor are shown as an example in Fig. 2b. For clarity on this figure, the $\theta' = 0$ radial arms have been omitted. The solid dots on the circles mark the points appropriate for the two Bahr rotation angles α_1 and α_2, and the Bahr skew angles β_1, β_2, β_3 and β_4 are then as shown (where β_3 and β_4 for α_2 correspond to β_1 and β_2 for α_1). Numerical details on the example of Fig. 2b are given in an Appendix below.

Note that deviation of the example from an ideal locally-distorted case of regional 2D induction is indicated by departure of the solid dots on the circles from forming diametrically opposite pairs. For an ideal case where the dots do form diametrically opposite pairs, it can be seen that $2\alpha_1$ and $2\alpha_2$ would differ by 180° and so α_1 and α_2 would differ by 90°. Then also it can be seen that

$$\beta_1 = \beta_4 \text{ and } \beta_2 = \beta_3$$

so that both α rotations of the impedance tensor produce measuring axes with the same alignments, and give the same results for the skew angles.

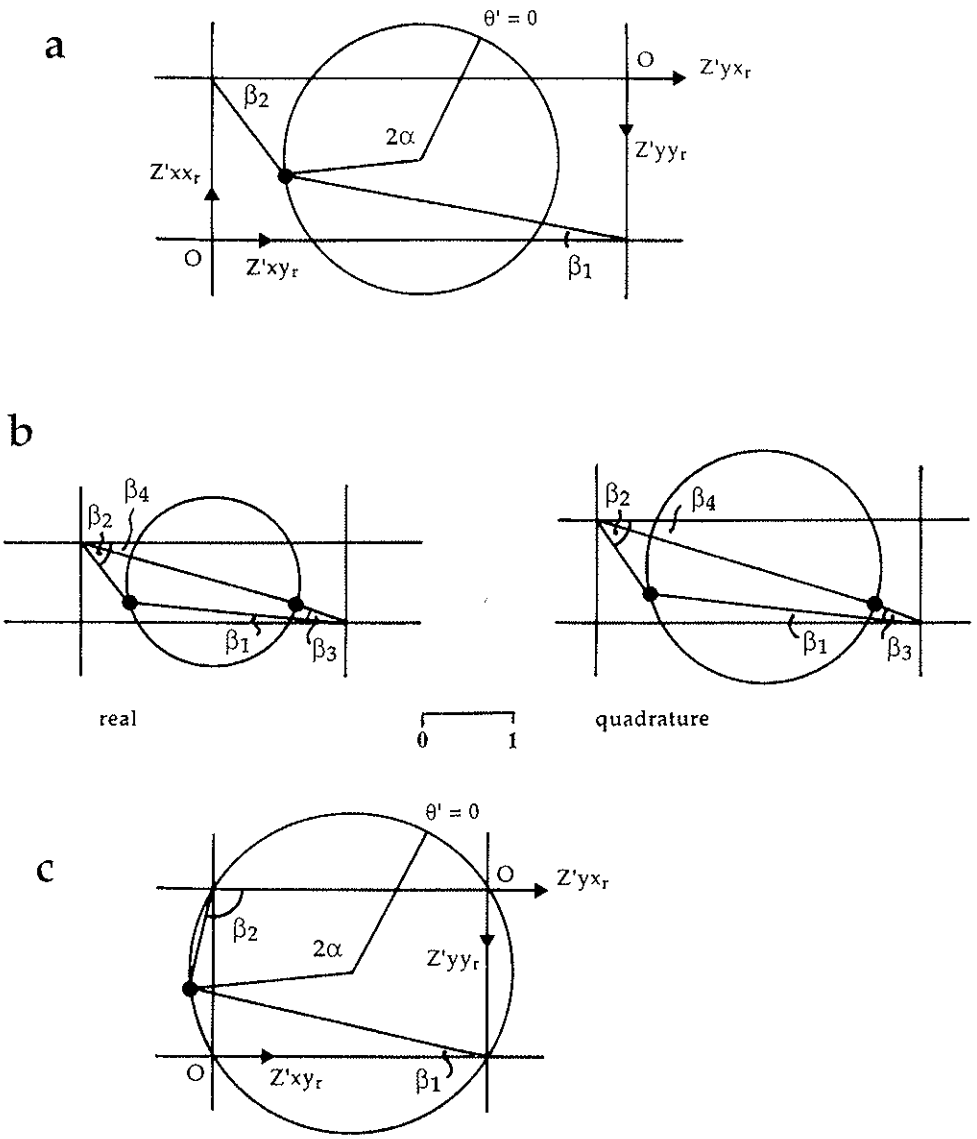

Fig. 2. (a) The Bahr rotation angle α and its related skew angles β_1 and β_2 as evident on a Mohr circle diagram. There will also be a second rotation angle (not shown). (b) Real and quadrature circles for an example impedance tensor. The solid dots on the circles mark Bahr's two rotation values α_1 and α_2. The Bahr skew angles, β_1 and β_2 for α_1, and β_3 and β_4 for α_2, are then as shown. Numerical data for this example are given in an Appendix below, and a scale for both real and quadrature circles is given on the figure. (c) The relationship $\beta_2 = \beta_1 + 90°$ shown for a case of strong 2D distortion or high anisotropy, where the circle goes through (or near) all the axis intersections.

Special cases may be of interest. For example, if there is no local distortion of a regional 2D situation, the $Z'xy_r$ and $Z'yx_r$ axes (as in Fig. 2a) move to be co-linear, with the centre of the circle then situated on them. Then, as can be seen,

$$\beta_1 = \beta_2 = 0$$

consistent with Bahr's analysis. The circle, with its centre on the horizontal axis, has a basic 2D form.

If, in contrast, high anisotropy or strong 2D distortion occurs, this circumstance will be apparent on the Mohr circle diagram by the circle going through (or near) every intersection of axes (LILLEY, 1993). Such a situation is shown in Fig. 2c. It follows immediately from the figure that

$$\beta_2 = \beta_1 + 90^\circ$$

consistent with Bahr's analysis (class 6 of BAHR, 1991).

4. Conclusions

The Mohr circle representation shows patterns and angles which may help an interpreter recognize certain characteristics in magnetotelluric impedance data. For one-dimensional data affected by simple static shift, circles for a range of frequencies will lie in a distinctive envelope. Depicting observed data by Mohr circles may thus immediately enable the identification of such static-shift problems.

More generally, in the analysis of a 3D impedance tensor the Bahr skew angles β_1 and β_2 (also described as the angular deviations of the telluric vectors) are shown directly by Mohr circle diagrams, once the Bahr rotation angles (α) are determined. Modern computer graphics also allow the demonstration of the α angles graphically, by displaying real and quadrature circles simultaneously and stepping out increments in the rotation angle dynamically.

The Bahr angles are important indicators of the dimensionality required to interpret data, and the circles give a visual method for identifying certain classes of local distortion without modelling or interpretation. Such graphical methods may add to the understanding which comes from numerical solutions alone.

The author acknowledges the benefit of discussion at the Eleventh Workshop on Electromagnetic Induction in the Earth, held at the Victoria University of Wellington, New Zealand, in August-September 1992. He thanks Karsten Bahr for discussion and correspondence, and the referees for valuable comments.

APPENDIX

Numerical Details of the Example in Fig. 2b.

The tensor given in Fig. 2b has numerical values (each having been multiplied by $T^{1/2}$ where T is in hr) of

$$\begin{bmatrix} 0.019, 0.006 & 0.608, 0.661 \\ -2.281, -2.988 & 0.853, 1.141 \end{bmatrix}.$$

The real Mohr circle thus has centre at coordinates

$$(Z'xy_r, Z'xx_r) = (1.44, 0.436)$$

and is of radius 0.936.

The quadrature Mohr circle has centre at coordinates

$$(Z'xy_q, Z'xx_q) = (1.824, 0.574)$$

and is of radius 1.286.

Bahr's rotation angles, calculated using Eq. (11) of his 1988 paper, are

$$\alpha_1 = -8^\circ \text{ and } \alpha_2 = 67^\circ$$

with associated skew angle values of

$$\beta_1 = 6^\circ,\ \beta_2 = 53^\circ,\ \beta_3 = 13^\circ \text{ and } \beta_4 = 18^\circ.$$

BAHR's (1991) regional skew value for the tensor is

$$\eta = 0.09$$

which is a small value by Bahr's criteria, implying validity of interpretation by a model of regional 2D induction, distorted locally.

A further point is that this example shows data for just one frequency for the purposes of illustration. An important characteristic to be checked in the analysis of data over a frequency range is that the angles obtained should be frequency-independent.

REFERENCES

BAHR, K., Interpretation of the magnetotelluric impedance tensor: regional induction and local telluric distortion, *Geophysics*, **62**, 119–127, 1988.

BAHR, K., Geological noise in magnetotelluric data: a classification of distortion types, *Phys. Earth Planet. Inter.*, **66**, 24–38, 1991.

JONES, A. G., Static shift of magnetotelluric data and its removal in a sedimentary basin environment, *Geophysics*, **53**, 967–978, 1988.

LILLEY, F. E. M., Diagrams for magnetotelluric data, *Geophysics*, **41**, 766–770, 1976.

LILLEY, F. E. M., Magnetotelluric analysis using Mohr circles, *Geophysics*, 1993 (in press).